European Journal of Nuclear Medicine and Molecular Imaging (2019) 46:206–216
https://doi.org/10.1007/s00259-018-4154-5

ORIGINAL ARTICLE

A prospective study of the feasibility of FDG-PET/CT imaging to quantify radiation-induced lung inflammation in locally advanced non-small cell lung cancer patients receiving proton or photon radiotherapy

Pegah Jahangiri[1] · Kamyar Pournazari[1] · Drew A. Torigian[1] · Thomas J. Werner[1] · Samuel Swisher-McClure[2] · Charles B. Simone II[3] · Abass Alavi[1]

Received: 8 May 2018 / Accepted: 29 August 2018 / Published online: 18 September 2018

Abstract

Purpose This prospective study assessed the feasibility of ^{18}F-2-fluoro-2-deoxy-D-glucose (FDG) positron emission tomography/computed tomography (PET/CT) to quantify radiation-induced lung inflammation in patients with locally advanced non-small cell lung cancer (NSCLC) who received radiotherapy (RT), and compared the differences in inflammation in the ipsilateral and contralateral lungs following proton and photon RT.

Methods Thirty-nine consecutive patients with NSCLC underwent FDG-PET/CT imaging before and after RT on a prospective study. A novel quantitative approach utilized regions of interest placed around the anatomical boundaries of the lung parenchyma and provided lung mean standardized uptake value (SUVmean), global lung glycolysis (GLG), global lung parenchymal glycolysis (GLPG) and total lung volume (LV). To quantify primary tumor metabolic response to RT, an adaptive contrast-oriented thresholding algorithm was applied to measure metabolically active tumor volume (MTV), tumor uncorrected SUVmean, tumor partial volume corrected SUVmean (tumor-PVC-SUVmean), and total lesion glycolysis (TLG). Parameters of FDG-PET/CT scans before and after RT were compared using two-tailed paired t-tests.

Results All tumor parameters after either proton or photon RT decreased significantly ($p < 0.001$). Among the 21 patients treated exclusively with proton RT, no significant increase in PVC-SUVmean or PVC-GLPG was observed in ipsilateral lungs after the PVC parameters of primary tumor were subtracted ($p = 0.114$ and $p = 0.453$, respectively). Also, there were no significant increases in SUVmean or GLG of contralateral lungs of patients who received proton RT ($p = 0.841$, $p = 0.241$, respectively). In contrast, among the nine patients who received photon RT, there was a statistically significant increase in PVC-GLPG of ipsilateral lung ($p < 0.001$) and in GLG of contralateral ($p = 0.036$) lung. In the subset of nine patients who received a combined proton and photon RT, there was a statistically significant increase in PVC-GLPG of ipsilateral lung ($p < 0.001$).

Conclusion Our data suggest less induction of inflammatory response in both the ipsilateral and contralateral lungs of patients treated with proton compared to photon or combined proton-photon RT.

Keywords FDG-PET/CT · Radiation pneumonitis · Lung cancer · Proton · Photon radiotherapy

Introduction

Lung cancer is the second most frequently diagnosed cancer and the most common cause of cancer death in the United States in both men and women. An estimated 234,030 new lung cancer cases (121,680 in men and 112,350 in women) will be diagnosed in 2018, and 154,050 deaths (83,550 in men and 70,500 in women) will result from lung cancer, representing 25% of all deaths from cancer in the US [1]. Radiation therapy (RT) is a major treatment option for lung cancer, including for unresectable locally advanced non–small cell lung cancer (NSCLC) [2, 3]. Concurrent

Charles B. Simone and Abass Alavi are both senior authors.

✉ Charles B. Simone, II
CharlesSimone@umm.edu

[1] Department of Radiology, University of Pennsylvania, Philadelphia, PA, USA

[2] Department of Radiation Oncology, University of Pennsylvania, Philadelphia, PA, USA

[3] Department of Radiation Oncology, University of Maryland School of Medicine, 22 S. Greene Street, Baltimore, MD 21201, USA

chemoradiotherapy (CCRT) is the current standard of care in this population and yields an absolute survival benefit at 5 years of 5% relative to sequential chemotherapy and RT [4, 5]. Thoracic RT can result in considerable risks of radiation-induced toxicities, including lung injuries such as radiation pneumonitis (RP) and pulmonary fibrosis, particularly among patients also receiving chemotherapy [6]. Therefore, major efforts must be made to improve therapeutic outcomes via delivering sufficient radiation dose to tumor while limiting the radiation-induced damage to normal lung tissues.

RP is a common and potentially fatal complication caused by a cascade of pro-inflammatory cytokines in patients receiving thoracic RT [7–11]. The inflammatory changes within both tumor and surrounding lung parenchyma vary in timing [12]. RP most typically manifests in the first few weeks to 6 months after RT completion, and is characterized by varying symptoms from a mild non-productive cough to more severe manifestations of fever, dyspnea, respiratory failure, and even death [13–15]. The risk of RP occurrence is determined by numerous factors such as delivered radiation dose and the volume of functional lung irradiated [16, 17]. A meta-analysis by Palma et al. reported that symptomatic pneumonitis and fatal pneumonitis occur in approximately 30% and 2% of patients receiving CCRT, respectively [8]. Management generally consists of corticosteroids for several weeks to months with a gradual taper to prevent rebound pneumonitis [18]. The occurrence of RP and treatment-related death remain a significant bottleneck to radiation dose escalation in lung cancer [19]. To date, there is no established means to predict the future onset of RP [20]. Therefore, there is a high demand for establishing an effective, reliable, noninvasive, and quantitative imaging method to assist in designation of at-risk patients and in facilitation of earlier RP diagnosis and treatment by modifying the RT plan or by early initiation of corticosteroids to alleviate the severity of symptoms.

RT may cause changes in the lung such as edema, cellular infiltration into airspaces, and thickening of alveolar walls. These changes may be quantified using anatomical and morphological imaging techniques such as computed tomography (CT) [21].

Photon and proton therapy are both RT techniques but with different characteristics. Photons have essentially no mass and no charge but are extremely penetrable and capable of delivering an irradiation dose through any kind of tissue. Photon therapy, therefore, actively exposes healthy tissues along the beam path in front of and behind the tumor to incidental irradiation [22].

Protons, which are heavy and charged particles characterized by a well-defined range of penetration, can deliver their maximum dose at a specified depth. Proton therapy generally has a more optimal dose delivery in comparison to photon therapy. This physical benefit comes from a central-axis depth-dose distribution pattern known as the Bragg peak. Proton therapy delivers precise radiation doses to a tumor while minimizing the dose to surrounding normal tissues. By providing minimal integral radiation dose to surrounding critical organs, proton therapy can allow for improvements in clinical outcomes in select cases by more safely and efficiently allowing for dose escalation [22–24]. Since proton RT has higher cost and more limited availability relative to other radiation modalities and is not currently approved for reimbursement by all insurance carriers in United States, there is a more limited clinical experience to demonstrate an improved efficacy of proton RT in lung cancer relative to photon RT [5].

In recent years, ^{18}F-2-fluoro-2-deoxy-D-glucose (FDG) positron emission tomography/computed tomography (PET/CT) has repeatedly been shown to provide improved sensitivity and specificity for determining the diagnosis and stage of lung cancer [25–27]. FDG-PET/CT imaging, as an objective and quantitative measurement, has also been utilized in RT treatment planning, risk stratification, prognostication, and response monitoring for locally advanced NSCLC [28–30]. Moreover, it has an emerging but integral role to assess the extent of pulmonary inflammation after thoracic RT, which manifests as increased FDG uptake in lung parenchyma [7, 16, 31].

As such, we conducted this prospective study to: (1) investigate the feasibility of using volumetric-based FDG-PET/CT parameters to quantify the extent of lung inflammation in patients with locally advanced NSCLC who received thoracic RT; and (2) compare the quantitative inflammatory differences in the ipsilateral and contralateral lungs following proton and photon RT.

Methods and materials

Study population

Following Institutional Review Board (IRB) approval for prospective data collection and image analysis with Health Insurance Portability and Accountability Act (HIPAA) waiver, this prospective study was performed at the Hospital of the University of Pennsylvania. This study enrolled a total of 39 analyzed patients. Patients were predominantly female (53.8%) with a median age of 67 years (range 45–82 years) at the time of diagnosis. They had predominantly stage IIIA (61.5%) or stage IIIB (30.7%) NSCLC. All patients had locally advanced NSCLC and were treated with definitive CCRT without surgical resection. In all cases, patients received 66.6 Gy in 1.8 Gy (CGE for proton therapy) daily fractions with concurrent platinum-based doublet chemotherapy. Twenty-one, nine, and nine patients received proton RT, photon RT, and combined proton and photon RT, respectively. All patients

underwent pre-RT and post-RT FDG-PET/CT at our institution. A total of 78 individual lungs (two from each subject) were evaluated overall for this study. Table 1 provides an overview of the cohort included and Table 2 shows the average dose of radiotherapy was given to each cohort. While preexisting COPD was a common diagnosis amount the study cohort, no other pulmonary pathology was reported about the patients. No acute pneumonia or other inflammatory conditions were identified, and no preexisting inflammatory lung conditions like interstitial lung disease were identified.

PET/CT image acquisition

All subjects fasted for at least 6 h before receiving 555 MBq (15 mCi) of FDG administered intravenously. They had to have serum glucose levels of less than 200 mg/dL just prior to radiotracer injection. Routine FDG-PET/CT scans were acquired using a 16-detector row LYSO whole-body PET/CT scanner with time-of-flight capabilities (Gemini TF; Philips Healthcare, Bothell, WA). The average interval time between FDG-PET/CT and the start of RT was 41 days (range 8–236 days), whereas the average interval time between completion of RT and post-treatment FDG-PET/CT was 101 days (range 75–179 days). The median time between the pre- and post-treatment FDG-PET/CT scans was 197 days (range 147–467 days). Although most PET scans were obtained at approximately 3 months following the completion of radiation therapy in the majority of patients, the time points used in this study were the real clinical time points. As such, the analysis was based on these real clinical practice time points that were available for each subject.

PET images were attained from the base of skull to the mid-thigh approximately 60 min after FDG injection for 3 min per bed position. Capabilities of the system included time-of-flight, normalization, attenuation, random, and scatter

Table 1 Patient cohort characteristics

	Proton RT	Photon RT	Combined Proton and Photon RT	*p* value
Number of patients	21	9	9	
Gender				**0.810**
Female	12	5	4	
Male	9	4	5	
Tumor type				**0.234**
Adenocarcinoma	13	3	4	
Squamous cell carcinoma	8	6	4	
Poorly differentiated carcinoma	0	0	1	
Stage				**0.221**
IB	1[a]	0	0	
IIA	0	0	1[b]	
IIB	0	0	1[b]	
IIIA	15	4	5	
IIIB	5	5	2	
Chemotherapy				**0.443**
Cisplatin	1	2	3	
Carboplatin	15	5	4	
Etoposide	5	4	4	
Taxol	12	5	4	
Other Chemotherapy	8	2	2	

[a] This subject with stage IB was diagnosed with an early stage non-small cell lung cancer but then presented following initial treatment with mediastinal nodal recurrence (yN2 and de facto stage III). As staging does not change after initial treatment, this patient is listed as stage IB despite being treated with definitive chemoradiation for what clinically was stage III disease

[b] The two patients with stage II disease both had nodal metastasis and were thus not candidates for stereotactic body radiation therapy. Furthermore, they were not medically operable candidates. As such, they were also treated with definitive chemoradiation. As per standard guidelines, all stage II patients who are not undergoing surgery are treated with definitive chemoradiation in the exact same way that stage III patients are treated. In fact, in the only phase III randomized trial of locally advanced non-small cell lung cancer currently open in NRG Oncology (RTOG 1308), all patients with stage II or III medically inoperable non-small cell lung cancer are eligible and treated in the same way

Table 2 The average irradiation dose to lungs and heart for each treatment cohort

	Proton RT	Photon RT	Combined proton and photon RT
Average dose (cGY) to ipsilateral lung	2825	2787	2784
Average dose (cGY) to contralateral lung	335	438	157
Average dose (cGY) to heart	755	1863	807

corrections. Image reconstruction was performed using a list-mode maximum-likelihood expectation-maximization algorithm with thirty-three ordered subsets and three iterations. Energy rescaled low dose CT images were used for attenuation correction of PET images. Slice thickness were utilized on PET and CT acquisition to allow for fusion.

PET/CT scans and quantification analysis

The PET/CT scan analysis and quantification for each patient was performed by dedicated image visualization and analysis OsiriX MD software (Pixmeo SARL, Bernex, Switzerland). A novel quantitative method was used to obtain the region of interest (ROI). ROIs were drawn manually around the anatomical margins of the lung parenchyma from apex to base on each transverse slice of the fused PET/CT images. The diaphragm, trachea, and mainstem bronchi were excluded, but the tumor within the lung were included. The sectional lung mean standardized uptake value (sSUVmean) and the sectional lung ROI area (sArea) were then measured for all individual slices. These values were exported to be used for statistical analysis (Fig. 1).

Full automation was not utilized in the current study. In fact, full automation is not that simple, and it depends on the types of case being assessed. In the future, it may be feasible to automate such methods to quantify lung diseases including lung inflammation automatically or semi-automatically. It is conceivable that a more automated method may be developed in the future; however, segmentation has its own challenges, and this would be in the domain of future research study.

The sectional lung volume (sLV) was obtained by multiplying the sectional area of ROI (cm^2) on the slice by the slice thickness. Then, by summing all of the sLVs, across all slices through the lung, the total lung volume (LV) was calculated (total LV= $\sum(sSUVmean * sArea)$). We measured LV in both of pre- and post-RT scans. The sectional lung glycolysis (sLG) was calculated by multiplying sLV and sSUVmean from each slice, and the global lung glycolysis (GLG) was calculated by summing of all the sLG from each individual lung slices across all slices throughout the lung (GLG= $\sum(sSUVmean * sLV)$). Finally, the lung SUVmean was calculated by dividing the GLG by the LV (Lung SUVmean= $\frac{GLG}{Total\ LV}$). The above described parameters included the normal lung parenchyma in addition to the primary tumor lesions. Total lesion glycolysis was then subtracted from GLG to calculate global lung parenchymal glycolysis (GLPG).

$$GLPG = GLG - TLG$$

To quantify tumor metabolic response to RT, metabolically active tumor volumes (MTV), tumor SUVs, and total lesion glycolysis (TLG) were measured. An adaptive contrast-oriented thresholding algorithm was utilized to measure these parameters, which permits delineation of the boundaries of lesions based on PET images. This modified adaptive thresholding delineation technique combines automatically determined background correction and local adaptive thresholding in an iterative algorithm model [23–26] (ROVER software; ABX, Radeberg, Germany). To compute partial volume correction (PVC), a local background PVC algorithm was used. The accuracy and reproducibility of these methods have previously been verified [32, 33].

To measure the extent of inflammation of the normal lung parenchyma in response to RT, (Fig. 1), the following formulas were used:

- Δ *Lung Parenchymal SUVmean* = [(post − RT GLG − post − RT TLG)/(post − RT LV − post − RT MTV)] − [(pre − RT GLG – pre − RT TLG)/(pre − RT LV − pre − RT MTV)]
- Δ *Lung Parenchymal PVC − SUVmean* = [(post − RT GLG − post − RT PVC − TLG)/(post − RT LV − post − RT MTV)] − [(pre − RT GLG – pre − RT PVC − TLG)/(pre − RT LV − pre − RT MTV)]
- Δ GLPG = (post − RT GLG − post − RT TLG) − (pre − RT GLG − pre − RT TLG)
- Δ PVC − GLPG = (post − RT GLG − post − RT PVC − TLG) − (pre − RT GLG − pre − RT PVC − TLG)

Statistical analyses

All statistical analyses were performed using IBM SPSS Statistics version 25.0 (IBM Corporation, Armonk, NY, USA). To summarize the variables of this study, descriptive statistics were calculated (means, standard deviations, 95% confidence intervals). Parameters of FDG-PET/CT scans pre- and post-RT were compared using paired t-tests. Differences were considered to be statistically significant when the two-tailed p value was less than 0.05.

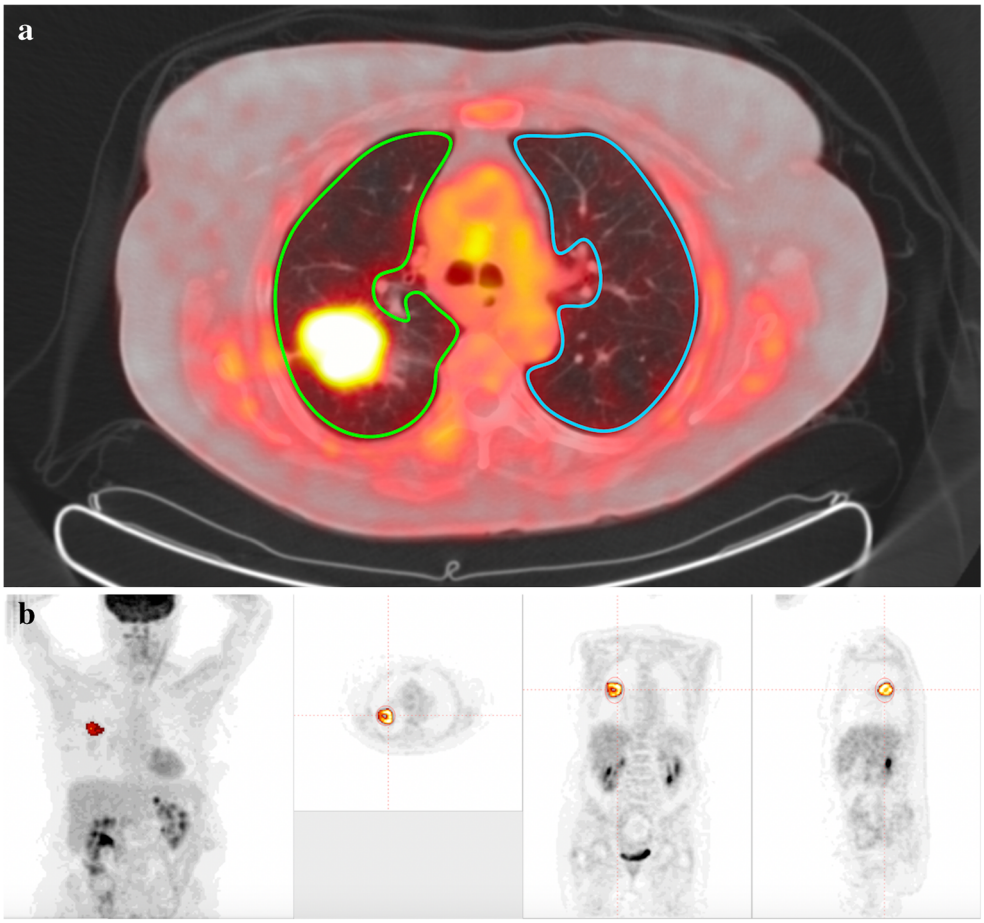

Fig. 1 Example of standardized uptake value and global lung glycolysis measurement and total lesion glycolysis in a patient with lung cancer. **a** Manually drawn ROIs are performed on fused PET/CT images on the ipsilateral and contralateral lungs (green and blue outlines, respectively) slice by slice axially from lung apex to base. Note FDG avid mass in right lung due to lung cancer. **b** Tumor regions (color overlay) are delineated with semiautomatic software. Total lesion glycolysis is then subtracted from GLG to calculate GLPG

Results

Inflammatory effects of RT upon the lungs

There were statistically significant differences in mean ipsilateral PVC-GLPG between pre-RT and post-RT PET/CT scans among patients receiving either photon RT ($p < 0.001$) or combined proton and photon RT ($p < 0.001$). In patients treated exclusively with proton RT, there was no significant difference in mean ipsilateral PVC-GLPG between pre-RT and post-RT PET/CT scans ($p = 0.453$) (Fig. 2).

In patients treated with photon RT, there was a significant increase in mean contralateral GLG from pre-RT to post-RT PET/CT ($p = 0.036$). However, there were no significant differences in mean contralateral GLG between pre-RT and post-RT PET/CT scans among patients receiving combined photon and proton RT ($p = 0.077$) or proton RT ($p = 0.241$) (Fig. 3).

In photon RT and combined photon and proton RT patients, there were significant increases in mean ipsilateral lung PVC-SUVmean from pre-RT to post-RT PET/CT scans ($p < 0.001$ and $p < 0.001$, respectively). In contrast, there was no significant difference in mean ipsilateral lung PVC-SUVmean between pre-RT and post-RT PET/CT scans in proton RT patients ($p = 0.114$) (Fig. 4).

There were no significant differences in mean contralateral lung SUVmean between pre-RT and post-RT PET/CT scans among patients receiving photon RT ($p = 0.643$), proton RT ($p = 0.841$), or combined photon and proton RT ($p = 0.679$) (Fig. 5). Table 3 shows a summary of the inflammatory effects of RT upon the ipsilateral and contralateral lungs.

Tumor response

In primary tumors, statistically significant decreases were observed in post-RT (proton, photon or combined proton-photon) MTV, SUVmax, uncorrected SUVmean, PVC-SUVmean, uncorrected TLG, and PVC-TLG (all $p < 0.001$). The decreases in PVC-TLG and tumor PVC-SUVmean were more obvious than uncorrected ones (ΔPVC-TLG -357.26 versus ΔTLG -252.92; ΔPVC-SUVmean −16.2 versus ΔSUVmean −10.19). All parameters related to tumor response are shown in Table 4.

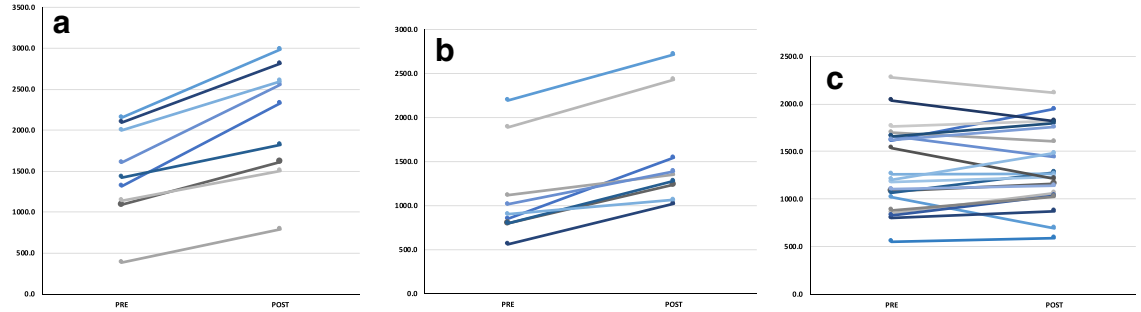

Fig. 2 Ipsilateral lung PVC-GLPG in patients **a** photon, **b** combined proton-photon or **c** proton RT

Discussion

FDG uptake is not tumor specific, as it occurs not only in areas of enhanced cellular metabolism due to tumor, but also in areas of enhanced cellular metabolism due to inflammation [34, 35]. In recent years, the application and study of FDG-PET/CT to assess and quantify lung inflammation in various types of disease conditions including chronic obstructive pulmonary disease (COPD), sarcoidosis, and interstitial lung disease has been rapidly evolving [36–38]. The primary goal of the current study was to quantify lung inflammation through FDG-PET/CT in NSCLC patients undergoing proton or photon RT. Our findings suggest a significant increase in inflammation in the affected lung, when treated with photon RT. In particular, both PVC-GLG and PVC-SUVmean values increased significantly in the ipsilateral lung following photon RT. In contrast, proton RT did not lead to similar such increases. For quantitative assessment of the inflammatory effects of RT from PET images, the changes based on GLG and SUVmean using partial volume correction showed significant increases, whereas the uncorrected changes were not statistically significant. This observation supports the importance of performing partial volume correction for the PET quantification of lung inflammation. This study is the first-of-its-kind to assess the feasibility of this approach by using different parameters; therefore, a power analysis was not quantifiable and is not appropriate at this stage. Despite this, we were able to show statistically significant differences that are biologically consistent. This methodology and preliminary results are being used for a future large-scale study that will include a power analysis.

The two primary factors determining the modality used was patient insurance status and disease extent. Due to its ability to better protect normal tissues, proton therapy was the default modality for most of our patients with locally advanced non-small cell lung cancer. However, some patients have health insurance that were less likely to approve proton therapy for lung cancer, and these patients were treated with photons. Additionally, patients who had large tumor volumes and/or harder to treat tumors were also more likely to receive proton therapy, as these patients were thought not to be as safely treatable with photon therapy. This is in keeping with other prior reports were proton therapy was used for larger tumors [39]. Selection bias may impacted our results, although this selection might have biased against proton therapy since larger tumors that were more likely to be treated with proton therapy required treatment with larger irradiation fields that might have led to higher inflammatory effects to the normal lungs.

RT is a major therapeutic modality that is used to treat many patients with lung cancer. Cell death and arrested mitosis arise from ionizing radiation-related deoxyribonucleic acid (DNA) damage and are accompanied by altered interactions between tumor and factors in the microenvironment including hypoxia, tumor microvasculature, and host immune cells [12]. Following RT, inflammatory changes, such as acute and subacute RP, as well as pulmonary fibrosis may also occur, the latter of which is more common in patients who suffer from acute RP [35, 40]. Therefore, the goal in RT treatment

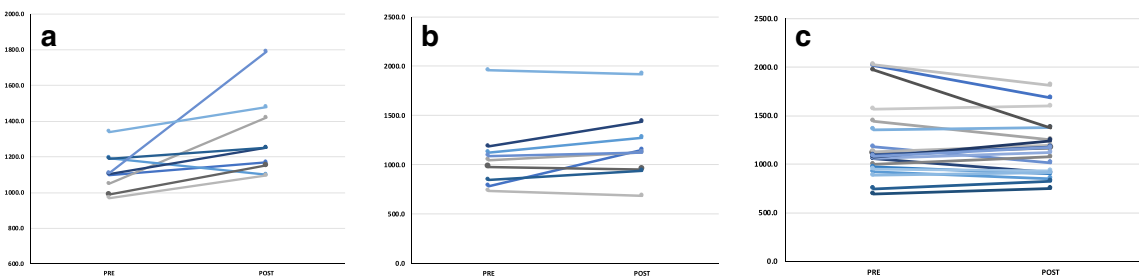

Fig. 3 Contralateral lung GLG in patients receiving **a** photon, **b** combined proton-photon or **c** proton RT

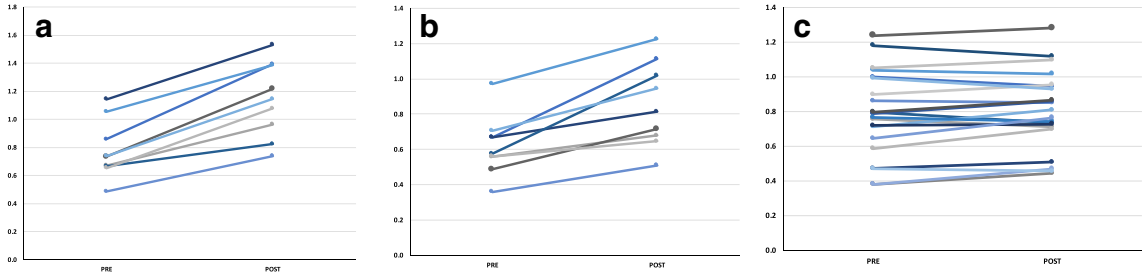

Fig. 4 Ipsilateral lung PVC-SUVmean in patients receiving **a** photon, **b** combined proton-photon or **c** proton RT

planning is to provide the highest therapeutic radiation dose to the sites of tumor while sparing the normal surrounding tissues from radiation dose as much as possible without exceeding specific organ at risk tolerances. Total radiation dose, fraction size, duration of the radiation course, the tumor location, and the irradiated volume are all factors that may modulate the frequency of adverse effects following RT [20, 35]. Findings of the Radiation Therapy Oncology Group (RTOG) in a large randomized trial on curative-intent treatment of patients with stage IIIA/IIIB NSCLC (RTOG 0617) showed that the overall survival after high-dose photon RT (74 Gy, 2 Gy per fraction) was worse than that after standard-dose RT (60 Gy, 2 Gy per fraction) (median survival of 20.3 months vs. 28.7 months) [19]. Higgins et al. reported improved survival for patients with stage II and III NSCLC treated with proton RT relative to photon RT [5].

Some researchers have studied the important role of FDG-PET/CT in assessing radiation-induced lung inflammation [7, 13, 16, 31, 41]. Marks et al. observed that inflammatory alterations in the lungs are noticeable on radiographic images of 30% to 90% of patients following 30 Gy RT to 70 Gy RT [42].

Because of the differential physics of charged particles and their interaction with matter compared to photons, proton RT allows higher radiation doses to be focused to regions within the tumor while minimizing the dose to surrounding organs at risk such as the heart, lung parenchyma, esophagus, spinal cord, and brachial plexus. Therefore, proton RT has been proposed as an advanced technology to reduce the risk of treatment-induced toxicities and to potentially improve the effectiveness of local tumor control and overall survival compared to photon RT in the treatment of patients with NSCLC [43]. Much retrospective and prospective clinical data have demonstrated the dosimetric advantage of proton RT in comparison with photon RT and have shown its safety and efficacy for treatment of NSCLC. In particular, proton RT offers the ability to decrease inflammation in the lungs, which may translate to a reduction in the occurrence of RP [22, 44, 45]. Our results support this finding, as we observed increases in lung GLG and SUVmean on post-treatment PET/CT after photon RT but not after proton RT, suggesting less induction of inflammatory response following proton RT.

The prompt diagnosis of radiation-induced lung injury may lead to more successful treatment of this potentially fatal toxicity. Existing clinical scoring systems are challenging to yield an accurate diagnosis in 28% to 48% of RP cases [46, 47]. In recent years, some studies have investigated quantitative parameters to assess RP. In one study, the relationship of the inflammatory changes of lung parenchyma in 73 consecutive patients with NSCLC receiving photon RT using FDG-PET/CT were assessed by Hicks et al. and compared with the metabolic response at tumor sites. They found an association between complete or partial tumor response and increased FDG uptake in normal lung tissue, suggesting a probable positive relationship between tumor radio-responsiveness and normal lung tissue radio-sensitiveness [41]. Guerrero et al. investigated the relationship between local radiation dose and RP in 36 patients with esophageal cancer. These patients underwent restaging FDG-PET/CT imaging almost six weeks after

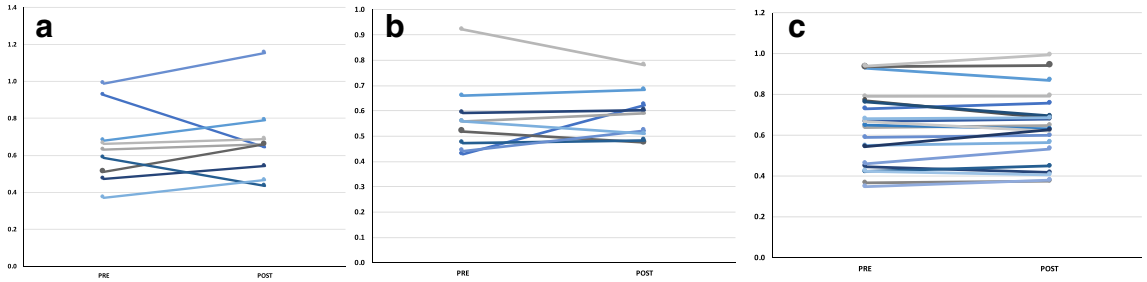

Fig. 5 Contralateral lung SUVmean in patients receiving **a** photon, **b** combined proton-photon or **c** proton RT

Table 3 Comparison of FDG-PET/CT (FDG-PET/CT: ^{18}F-2-fluoro-2-deoxy-D-glucose positron emission tomography/computed tomography) parameters before and after treatment in patients receiving proton, photon, or combined proton and photon RT

Lung	FDG-PET/CT parameter	Group	Mean absolute change	Mean relative change (%)	*p* value*
Ipsilateral	ΔSUVmean[a]	Proton	0.01	1.38%	0.463
Ipsilateral	ΔSUVmean	Photon	0.26	29.22%	**<0.001**
Ipsilateral	ΔSUVmean	Combined	0.16	23.22%	**0.003**
Ipsilateral	ΔPVC[b]-SUVmean	Proton	0.02	2.80%	0.114
Ipsilateral	ΔPVC-SUVmean	Photon	0.36	46.75%	**<0.001**
Ipsilateral	ΔPVC-SUVmean	Combined	0.23	36.53%	**<0.001**
Ipsilateral	ΔGLPG[c]	Proton	−44.77 cc	−3.18%	0.325
Ipsilateral	ΔGLPG	Photon	489.03 cc	30.14%	**<0.001**
Ipsilateral	ΔGLPG	Combined	297.28 cc	23.42	**0.001**
Ipsilateral	ΔPVC-GLPG	Proton	31.71 cc	2.40%	0.453
Ipsilateral	ΔPVC-GLPG	Photon	645.70 cc	44.05%	**<0.001**
Ipsilateral	ΔPVC-GLPG	Combined	419.97 cc	37.09%	**<0.001**
Contralateral	ΔSUVmean	Proton	0.00	0.30%	0.841
Contralateral	ΔSUVmean	Photon	0.02	3.67%	0.643
Contralateral	ΔSUVmean	Combined	0.01	2.31%	0.679
Contralateral	ΔGLG[d]	Proton	−46.90 cc	−3.89%	0.241
Contralateral	ΔGLG	Photon	185.95 cc	16.68%	**0.036**
Contralateral	ΔGLG	Combined	95.74 cc	8.83%	0.077

RT: Radiotherapy

[a] SUV: Standardized Uptake Value

[b] PVC: partial volume corrected

[c] GLPG: Global Lung Parenchymal Glycolysis

[d] GLG: Global Lung Glycolysis

*Significant *p* values are displayed in bold

combined chemotherapy and photon RT. The study showed a linear relationship between local radiation dose and the normalized FDG uptake in the lung after treatment as a marker of the development of RP. More interestingly, the investigators reported discrepancies in the slope of this relationship among individual patients, which was not impacted by the time interval (1–3 months) between RT completion and PET imaging and by the irradiated LV. As such, they concluded that the response slope can be applied as a metric for the quantification of individual intensity of RP [31]. Further study by Echeverria et al. assessed proton RT–induced RP in 100 patients with esophageal cancer and showed a positive correlation between symptomatic patients and radiation dose response on FDG-PET/CT [7]. Hart et al. retrospectively studied 101 patients with esophageal cancer, where they evaluated the pulmonary metabolic activity 3–12 weeks after photon RT in relation to clinical symptoms of RP based on a scoring system. They observed a statistically significant correlation between the increase in radiation dose and RP clinical symptoms ($p = 0.032$), as well as between increase in FDG uptake and RP clinical symptoms ($p = 0.033$) [16].

Yet, qualitative visual analysis of PET images is still the principal methodology used for the assessment of RP in clinical practice. Visual assessment relies on the contrast between FDG-avid areas and areas with lower FDG uptake. This method is mostly utilized in the interpretation of clinical FDG-PET/CT studies to detect lesions with high glycolytic activity relative to background related in part to an increased retention of FDG-6-phosphate in cells [48]. Metabolically active confounders of lung inflammation following RT may be encountered on FDG-PET, including acute infection, residual or recurrent malignancy, esophagitis, and pericarditis, amongst others [35].

It is often difficult to establish a ground truth in many cases, yet despite this limitation, we have developed a new methodology that can be applied to any PET/CT in similar fashion which would minimize random errors and increase reproducibility. However, despite this limitation, PET is already used in clinical practice routinely to measure disease such as cancer where there is also in many cases a lack of a cortical reference standard, and yet it is still considered to be clinically useful and changes management in a large proportion of patients. In this initial study, the methodology we have applied to quantify the disease was performed similarly in all the cases to standardize our approach, which should minimize random errors. In fact, in some sense reproducing the way the cases were assessed is an important factor of this study beyond the absolute accuracy of our findings. This can serve as the basis for future larger-scale studies, because our current study is a

Table 4 Tumor metabolic response parameters in all subjects

FDG-PET/CT[a] parameter	Mean absolute change	Mean relative change (%)	*p* value*
All Patients ($n = 39$)			
ΔMTV[b] cc	−32.07	−89.3%	**<0.001**
ΔSUVmax[c]	−15.79	−90.1%	**<0.001**
ΔSUVmean	−10.19	−88.9%	**<0.001**
ΔPVC-SUVmean	−16.2	−91.3%	**<0.001**
ΔTLG[d] cc	−252.92	−92.4%	**<0.001**
ΔPVC[e]-TLG cc	−357.3	−92.0%	**<0.001**
Patients received proton RT ($n = 21$)			
ΔMTV cc	−24.64	−83.7%	**<0.001**
ΔSUVmax	−13.85	−83.4%	**<0.001**
ΔSUVmean	−15.12	−88.9%	**<0.001**
ΔPVC-SUVmean	−161.85	−84.3%	**<0.001**
ΔTLG cc	−234.52	−84.1%	**<0.001**
ΔPVC-TLG cc			**<0.001**
Patients received photon RT ($n = 9$)			
ΔMTV	−33.17	−100%	**0.024**
ΔSUVmax	−24.63	−100%	**0.003**
ΔSUVmean	−15.34	−100%	**0.003**
ΔPVC-SUVmean	−23.72	−100%	**0.006**
ΔTLG cc	−399.69	−100%	**0.018**
ΔPVC-TLG cc	−556.36	−100%	**0.016**
Patients received combined proton-photon RT (n = 9)			
ΔMTV cc	−48.30	−89.8%	**0.026**
ΔSUVmax	−11.47	−82.5%	**<0.001**
ΔSUVmean	−6.01	−80.9%	**0.002**
ΔPVC-SUVmean	−11.19	−82.9	**0.001**
ΔTLG cc	−318.66	−94.2%	**0.017**
ΔPVC-TLG cc	−444.53	−93.5%	**0.017**

[a] FDG-PET/CT: ^{18}F-2-fluoro-2-deoxy-D-glucose positron emission tomography/computed tomography

[b] MTV: Metabolic Tumor Volume

[c] SUV: Standardized Uptake Value

[d] TLG: Total Lesion Glycolysis

[e] PVC: partial volume corrected

*Significant *p* values are displayed in bold

preliminary study, and this is the first time such an approach has been conducted. Not having a reference standard makes the research challenging. Yet, we have applied the logical and consistent methodology in every case and showed the systematic difference between the proton and photon groups, and these need to be further validated with large-scale studies and show correlations with outcomes.

A retrospective pilot study by Abdulla et al. evaluated FDG uptake in 20 consecutive patients with stage III NSCLC who were treated with photon RT. In order to exclusively assess lung parenchyma, they subtract sites of tumor uptake from total lung uptake on FDG-PET/CT and found statistically significant increases in GLPG and lung parenchyma SUVmean in the ipsilateral lung, whereas there were no significant changes in the contralateral lung. Furthermore, they reported that partial volume correction is important to utilize when assessing lung inflammation [13].

There are several limitations of our study. One limitation is the relatively small sample size, although this is mitigated by intra-patient comparisons before and after RT and the homogeneity in treatment and imaging of the prospectively enrolled patients. Another one is the inability to conclusively correlate our findings to clinical acute and late pulmonary toxicity data and of quality-of-life outcomes given the limited sample size and the even more limited number of adverse radiation-induced toxicities. Such an analysis is planned as the primary endpoint of a future larger scale study. We did not explore radiomics in this preliminary study, but it may have potential

added valued to further discriminate inflammation from non-inflamed lung. Radiomics has recently been reported to have some value for improved characterization of cancer lesions, although there is some redundancy with currently available more global metrics such as SUV and TLG.

Chemotherapeutic agents can have inflammatory side effects upon the lung that may manifest as drug toxicity that can be detectable on chest CT scans. In this particular study, it was not feasible to separate out those two effects. However, in our study all patients received chemotherapy. While it is possible that some of the inflammations in the lungs may have been related to this, this should have been balanced out between the photon and proton patients. It is possible that some of the detected lung inflammation maybe related to actual chemotherapeutic agents. Of note, however, no patient in this study developed a more generally lung pathology outside of the treatment field, further making primary chemotherapy-induced lung morbidity less likely. Also of note, no historically known highly pulmonary toxic chemotherapy agents, such as bleomycin and gemcitabine, were administered to any patient in this study. In summary, we have demonstrated the feasibility of quantifying lung inflammation in patients with locally-advanced NSCLC following thoracic RT in a prospective clinical trial by using volume-based FDG-PET/CT parameters. Our results also revealed significant increases in lung inflammation on post-treatment FDG-PET/CT after photon RT, whereas such increases were not identified in patients receiving proton RT, suggesting less induction of inflammatory response in both the ipsilateral and contralateral lungs of patients undergoing concurrent chemoradiation with proton RT. FDG-PET/CT may, therefore, be useful for early detection and treatment of radiation-induced lung toxicities in the setting of RT. Future larger scale studies involving comparisons of FDG-PET/CT findings with clinical assessments of RP and measures of patient clinical outcomes are necessary for validation of our current findings, and to determine whether FDG-PET/CT may be cost-effective for improved prevention or earlier treatment of radiation-induced lung toxicity.

Funding This trial was funded, in part, by the McNichol Lung Cancer Research Philanthropy Fund.

Compliance with ethical standards

Conflict of Interest All authors declare that they have no conflict of interest.

Ethical approval All procedures performed in studies involving human participants were in accordance with the ethical standards of the University of Pennsylvania IRB and with the 1964 Helsinki Declaration and its later amendments or comparable ethical standards.

Informed consent Informed consent was obtained from all individual participants included in the study.

References

1. Siegel RL, Miller KD, Jemal A. Cancer statistics, 2017. CA Cancer J Clin. 2017;67:7–30. https://doi.org/10.3322/caac.21387.
2. Hardcastle N, Hofman MS, Hicks RJ, Callahan J, Kron T, MacManus MP, et al. Accuracy and utility of deformable image registration in 68 Ga 4D PET/CT assessment of pulmonary perfusion changes during and after lung radiation therapy. Int J Radiat Oncol Biol Phys. 2015;93:196–204.
3. Ulaner GA, Lyall A. Identifying and distinguishing treatment effects and complications from malignancy at FDG PET/CT. Radiographics. 2013;33:1817–34.
4. Verma V, Simone CB 2nd, Werner-Wasik M. Acute and late toxicities of concurrent chemoradiotherapy for locally-advanced non-small cell lung cancer. Cancers. 2017;9:120.
5. Higgins KA, O'Connell K, Liu Y, Gillespie TW, McDonald MW, Pillai RN, et al. National Cancer Database analysis of proton versus photon radiation therapy in non-small cell lung cancer. Int J Radiat Oncol Biol Phys. 2017;97:128–37.
6. Zhang X-J, Sun J-G, Sun J, Ming H, Wang X-X, Wu L, et al. Prediction of radiation pneumonitis in lung cancer patients: a systematic review. J Cancer Res Clin Oncol. 2012;138:2103–16.
7. Echeverria AE, McCurdy M, Castillo R, Bernard V, Ramos NV, Buckley W, et al. Proton therapy radiation pneumonitis local dose–response in esophagus cancer patients. Radiother Oncol. 2013;106:124–9.
8. Palma DA, Senan S, Tsujino K, Barriger RB, Rengan R, Moreno M, et al. Predicting radiation pneumonitis after chemoradiation therapy for lung cancer: an international individual patient data meta-analysis. Int J Radiat Oncol Biol Phys. 2013;85:444–50.
9. Castillo R, Pham N, Ansari S, Meshkov D, Castillo S, Li M, et al. Pre-radiotherapy FDG PET predicts radiation pneumonitis in lung cancer. Radiat Oncol. 2014;9:74.
10. Simone CB 2nd. Thoracic radiation normal tissue injury. Semin Radiat Oncol. 2017:370–7. Elsevier
11. Valdes G, Solberg TD, Heskel M, Ungar L, Simone CB 2nd. Using machine learning to predict radiation pneumonitis in patients with stage I non-small cell lung cancer treated with stereotactic body radiation therapy. Phys Med Biol. 2016;61:6105.
12. Weller A, O'Brien M, Ahmed M, Popat S, Bhosle J, McDonald F, et al. Mechanism and non-mechanism based imaging biomarkers for assessing biological response to treatment in non-small cell lung cancer. Eur J Cancer. 2016;59:65–78.
13. Abdulla S, Salavati A, Saboury B, Basu S, Torigian DA, Alavi A. Quantitative assessment of global lung inflammation following radiation therapy using FDG PET/CT: a pilot study. Eur J Nucl Med Mol Imaging. 2014;41:350–6.
14. Mac Manus MP, Ding Z, Hogg A, Herschtal A, Binns D, Ball DL, et al. Association between pulmonary uptake of fluorodeoxyglucose detected by positron emission tomography scanning after radiation therapy for non–small-cell lung cancer and radiation pneumonitis. Int J Radiat Oncol Biol Phys. 2011;80:1365–71.
15. McCurdy MR, Castillo R, Martinez J, Al Hallack MN, Lichter J, Zouain N, et al. [18 F]-FDG uptake dose–response correlates with radiation pneumonitis in lung cancer patients. Radiother Oncol. 2012;104:52–7.
16. Hart JP, McCurdy MR, Ezhil M, Wei W, Khan M, Luo D, et al. Radiation pneumonitis: correlation of toxicity with pulmonary metabolic radiation response. Int J Radiat Oncol Biol Phys. 2008;71:967–71.
17. Anthony GJ, Cunliffe A, Castillo R, Pham N, Guerrero T, Armato SG, et al. Incorporation of pre-therapy 18F-FDG uptake data with CT texture features into a radiomics model for radiation pneumonitis diagnosis. Med Phys. 2017.

18. Rodrigues G, Lock M, D'Souza D, Yu E, Van Dyk J. Prediction of radiation pneumonitis by dose–volume histogram parameters in lung cancer—a systematic review. Radiother Oncol. 2004;71: 127–38.
19. Bradley JD, Paulus R, Komaki R, Masters G, Blumenschein G, Schild S, et al. Standard-dose versus high-dose conformal radiotherapy with concurrent and consolidation carboplatin plus paclitaxel with or without cetuximab for patients with stage IIIA or IIIB non-small-cell lung cancer (RTOG 0617): a randomised, two-by-two factorial phase 3 study. Lancet Oncol. 2015;16:187–99.
20. Houshmand S, Boursi B, Salavati A, Simone CB 2nd, Alavi A. Applications of Fluorodeoxyglucose PET/computed tomography in the assessment and prediction of radiation therapy–related complications. PET Clin. 2015;10:555–71.
21. Abravan A, Knudtsen IS, Eide HA, Løndalen AM, Helland Å, van Luijk P, et al. A new method to assess pulmonary changes using 18F-fluoro-2-deoxyglucose positron emission tomography for lung cancer patients following radiotherapy. Acta Oncol. 2017:1–7.
22. Grutters JP, Kessels AG, Pijls-Johannesma M, De Ruysscher D, Joore MA, Lambin P. Comparison of the effectiveness of radiotherapy with photons, protons and carbon-ions for non-small cell lung cancer: a meta-analysis. Radiother Oncol. 2010;95:32–40.
23. Shioyama Y, Tokuuye K, Okumura T, Kagei K, Sugahara S, Ohara K, et al. Clinical evaluation of proton radiotherapy for non–small-cell lung cancer. Int J Radiat Oncol Biol Phys. 2003;56:7–13.
24. Simone CB 2nd, Rengan R. The use of proton therapy in the treatment of lung cancers. Cancer J. 2014;20:427–32.
25. Chin R Jr, Ward R, Keyes J, Choplin RH, Reed JC, Wallenhaupt S, et al. Mediastinal staging of non-small-cell lung cancer with positron emission tomography. Am J Respir Crit Care Med. 1995;152: 2090–6.
26. Sazon D, Santiago SM, Soo Hoo G, Khonsary A, Brown C, Mandelkern M, et al. Fluorodeoxyglucose-positron emission tomography in the detection and staging of lung cancer. Am J Respir Crit Care Med. 1996;153:417–21.
27. Vanuytsel LJ, Vansteenkiste JF, Stroobants SG, De Leyn PR, De Wever W, Verbeken EK, et al. The impact of 18 F-fluoro-2-deoxy-D-glucose positron emission tomography (FDG-PET) lymph node staging on the radiation treatment volumes in patients with non-small cell lung cancer. Radiother Oncol. 2000;55:317–24.
28. Salavati A, Duan F, Snyder BS, Wei B, Houshmand S, Khiewvan B, et al. Optimal FDG PET/CT volumetric parameters for risk stratification in patients with locally advanced non-small cell lung cancer: results from the ACRIN 6668/RTOG 0235 trial. Eur J Nucl Med Mol Imaging. 2017:1–15.
29. Simone CB 2nd, Houshmand S, Kalbasi A, Salavati A, Alavi A. PET-based thoracic radiation oncology. PET Clin. 2016;11:319–32.
30. Geiger GA, Kim MB, Xanthopoulos EP, Pryma DA, Grover S, Plastaras JP, et al. Stage migration in planning PET/CT scans in patients due to receive radiotherapy for non–small-cell lung cancer. Clin Lung Cancer. 2014;15:79–85.
31. Guerrero T, Johnson V, Hart J, Pan T, Khan M, Luo D, et al. Radiation pneumonitis: local dose versus [18 F]-fluorodeoxyglucose uptake response in irradiated lung. Int J Radiat Oncol Biol Phys. 2007;68:1030–5.
32. Torigian DA, Lopez R, Alapati S, Bodapati G, Hofheinz F, Saboury B, et al. Feasibility and performance of novel software to quantify metabolically active volumes and 3D partial volume corrected SUV and metabolic volumetric products of spinal bone marrow metastases on 18F-FDG-PET/CT. Hell J Nucl Med. 2011;14:8–14.
33. Hofheinz F, Dittrich S, Pötzsch C, Van Den Hoff J. Effects of cold sphere walls in PET phantom measurements on the volume reproducing threshold. Phys Med Biol. 2010;55:1099.
34. Metser U, Even-Sapir E. Increased 18 F-fluorodeoxyglucose uptake in benign, nonphysiologic lesions found on whole-body positron emission tomography/computed tomography (PET/CT): accumulated data from four years of experience with PET/CT. Semin Nucl Med: 2007:206–22. Elsevier.
35. Hassaballa HA, Cohen ES, Khan AJ, Ali A, Bonomi P, Rubin DB. Positron emission tomography demonstrates radiation-induced changes to nonirradiated lungs in lung cancer patients treated with radiation and chemotherapy. Chest. 2005;128:1448–52.
36. Kwee TC, Torigian DA, Alavi A. Nononcological applications of positron emission tomography for evaluation of the thorax. J Thorac Imaging. 2013;28:25–39.
37. Subramanian DR, Jenkins L, Edgar R, Quraishi N, Stockley RA, Parr DG. Assessment of pulmonary neutrophilic inflammation in emphysema by quantitative positron emission tomography. Am J Respir Crit Care Med. 2012;186:1125–32.
38. Torigian DA, Dam V, Chen X, Saboury B, Udupa JK, Rashid A, et al. In vivo quantification of pulmonary inflammation in relation to emphysema severity via partial volume corrected (18) F-FDG-PET using computer-assisted analysis of diagnostic chest CT. Hell J Nucl Med. 2013;16:12–8.
39. Liao Z, Lee JJ, Komaki R, Gomez DR, O'Reilly MS, Fossella FV, et al. Bayesian adaptive randomization trial of passive scattering proton therapy and intensity-modulated photon radiotherapy for locally advanced non–small-cell lung cancer. J Clin Oncol. 2018.
40. Mazeron R, Etienne-Mastroianni B, Pérol D, Arpin D, Vincent M, Falchero L, et al. Predictive factors of late radiation fibrosis: a prospective study in non–small cell lung cancer. Int J Radiat Oncol Biol Phys. 2010;77:38–43.
41. Hicks RJ, Mac Manus MP, Matthews JP, Hogg A, Binns D, Rischin D, et al. Early FDG-PET imaging after radical radiotherapy for non–small-cell lung cancer: inflammatory changes in normal tissues correlate with tumor response and do not confound therapeutic response evaluation. Int J Radiat Oncol Biol Phys. 2004;60:412–8.
42. Marks LB, Spencer DP, Bentel GC, Ray SK, Sherouse GW, Sontag MR, et al. The utility of SPECT lung perfusion scans in minimizing and assessing the physiologic consequences of thoracic irradiation. Int J Radiat Oncol Biol Phys. 1993;26:659–68.
43. Chang JY, Jabbour SK, De Ruysscher D, Schild SE, Simone CB 2nd, Rengan R, et al. Consensus statement on proton therapy in early-stage and locally advanced non–small cell lung cancer. Int J Radiat Oncol Biol Phys. 2016;95:505–16.
44. Chang JY, Zhang X, Wang X, Kang Y, Riley B, Bilton S, et al. Significant reduction of normal tissue dose by proton radiotherapy compared with three-dimensional conformal or intensity-modulated radiation therapy in stage I or stage III non–small-cell lung cancer. Int J Radiat Oncol Biol Phys. 2006;65:1087–96.
45. Chang JY, Li H, Zhu XR, Liao Z, Zhao L, Liu A, et al. Clinical implementation of intensity modulated proton therapy for thoracic malignancies. Int J Radiat Oncol Biol Phys. 2014;90:809–18.
46. Kocak Z, Evans ES, Zhou S-M, Miller KL, Folz RJ, Shafman TD, et al. Challenges in defining radiation pneumonitis in patients with lung cancer. Int J Radiat Oncol Biol Phys. 2005;62:635–8.
47. Yirmibesoglu E, Higginson DS, Fayda M, Rivera MP, Halle J, Rosenman J, et al. Challenges scoring radiation pneumonitis in patients irradiated for lung cancer. Lung Cancer. 2012;76:350–3.
48. Houshmand S, Salavati A, Hess S, Werner TJ, Alavi A, Zaidi H. An update on novel quantitative techniques in the context of evolving whole-body PET imaging. PET Clin. 2015;10:45–58.